Preparation of well-ordered cobalt nanostructures on Au(111)

Christian Tölkes, Peter Zeppenfeld, Michael A. Krzyzowski, Rudolf David, and George Comsa
Institut für Grenzflächenforschung und Vakuumphysik, Forschungszentrum Jülich, D-52425 Jülich, Germany
(Received 24 September 1996)

Nucleation and growth of cobalt adlayers on the reconstructed Au(111) surface at room temperature have been investigated by thermal energy helium-atom scattering experiments. The specular helium intensity provides information about the growth mode and the change in step height during Co epitaxy. Helium diffraction spectra further reveal the preferential nucleation of small Co clusters and the formation of long-range ordered zero- and one-dimensional Co structures. [S0163-1829(97)02020-1]

I. INTRODUCTION

The preparation of individual or periodic structures on solid surfaces at nanoscopic scales has become more and more important during the last years. Such ''nanostructures'' are expected to exhibit interesting physical and chemical properties.[1] Nanostructures can be produced by direct methods like atom manipulation using a scanning tunneling microscope (STM) (Refs. 2–5) and by growth. The structures obtained by growth can again be subdivided into thermodynamically and kinetically grown ones. In the latter case, the growth of the adsorbate is determined by heterogeneous nucleation at intrinsic defects on the substrate; these defects can be, for instance, steps on a vicinal surface[6] or particular sites on a reconstructed surface.[7] To find the right growth conditions for the preparation of well-defined nanostructures is not straightforward. Many parameters, such as the deposition method, temperature and rate, or the annealing procedure after deposition have to be evaluated in order to obtain a narrow size and distance distribution.

The interest in the epitaxial system Co/Au(111) is due to the fact that the combination of a ferromagnetic with a noncorrosive substrate material could play an important role in the search for data storage media. For this reason many studies have been performed on this system using a variety of different techniques like transmission electron diffraction,[8] x-ray diffraction,[9,10] reflection high-energy electron diffraction,[10] STM,[11] Auger electron spectroscopy (AES) or scanning electron microscopy with polarization analysis.[12] Only the STM studies of Voigtländer, Meyer, and Awen[11] dealt with submonolayer coverages and the influence of the Au(111) reconstruction on nucleation and submonolayer growth. Co atoms deposited at room temperature were found to nucleate preferentially at the ''elbows'' of the Au(111) reconstruction, similar to nickel[13] and iron atoms.[14] The step height of the Co islands as measured by STM corresponds to twice the distance of two adjacent Co(0001) lattice planes. On the background of these experiments we have looked for the mechanism of the formation of the Co double-layer islands and their influence on the growth mode of the subsequent layers. The exclusive surface sensitivity of thermal energy helium-atom scattering (TEAS) turned out to be very helpful for the investigation of these phenomena.

II. EXPERIMENT

The experiments have been performed in an UHV helium scattering apparatus at a base pressure of 5×10^{-11} mbar. The system is equipped with a supersonic helium nozzle beam, a four-grid low-energy electron-diffraction optics and a quadrupole mass spectrometer for residual gas analysis. The apparatus is described in detail in Ref. 15. Cobalt (impurity concentration $<10^{-4}$) was evaporized from a thin rod ($\sim$2 mm in diameter) by electron-impact heating. The purity of the deposition material and of the deposition process turned out to be essential for the reproducibility of the results. The deposition rate could be kept constant within $\pm10\%$ by monitoring the Co ion flux. During evaporation, the pressure in the main chamber did not exceed 1×10^{-10} mbar. The sample temperature T can be varied from 20 to 1200 K.

The Au(111) sample was cut from a gold single crystal whose contamination was less than 10^{-5}. The misorientation of the crystal against the (111) direction was less than 0.1°. After cleavage and polishing the sample was transferred into the UHV chamber and cleaned *in situ* by repeated cycles of argon-ion bombardment ($E_{Ar^+}=700$ eV) followed by annealing at $T=800$ K. This procedure had to be repeated after each deposition experiment to remove the deposited Co adlayers from the Au(111) surface.

The clean Au(111) surface exhibits a characteristic reconstruction pattern, as displayed in Fig. 1. The STM image clearly shows the pairs of parallel double ridges running across the surface. Because of the regular arrangement of the ''elbows'' this structure is often called a ''herringbone'' or ''chevron'' reconstruction. Its rectangular unit cell is given by the elbow distances $L_C\simeq73$ Å in the [112] direction and $L_K\simeq324$ Å in the [110] direction.[16] In the following, we denote by L_D the distance between neighboring double ridges perpendicular to their axis (see Fig. 1; $L_D=\sqrt{3}L_C/2\simeq63$ Å). Inside the double ridges a stacking fault leads to hcp stacking (A), in contrast to ordinary fcc stacking outside the ridges (B).[13,17] This structure appears in three equivalent orientations on the surface rotated by 120° against each other.

III. RESULTS AND DISCUSSION

A. Growth mode

Figure 2 shows a *deposition curve* of Co/Au(111) taken at room temperature, i.e., the dependence of the specularly

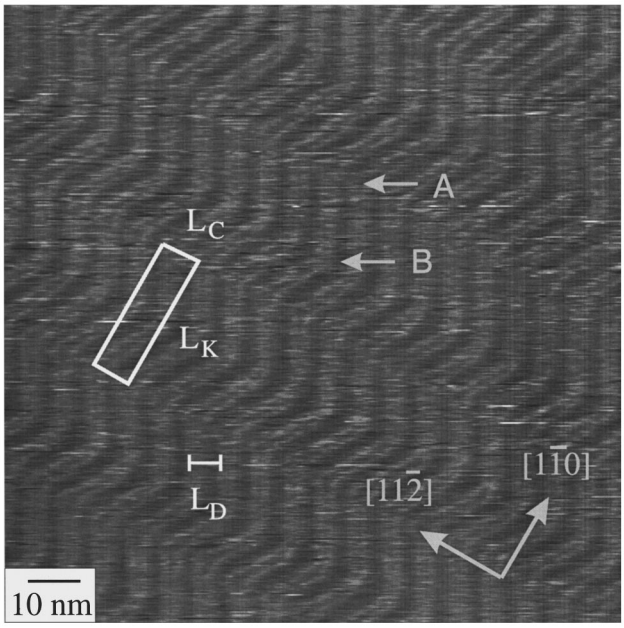

FIG. 1. STM image of the clean Au(111) surface at room temperature (Ref. 30). The unit cell of the reconstruction is marked by the white rectangle.

reflected helium intensity I on deposition time t. In all experiments described in this paper, the coverage Θ is defined as the number of deposited atoms per surface atom of the substrate. Since the deposition rate R was kept constant and the sticking coefficient can be assumed to be unity, $\Theta = Rt$. The details of the deposition process that specular helium scattering can detect depend strongly on the interference condition, i.e., on the total scattering angle χ and the helium wavelength λ. For *antiphase* scattering, helium beams scattered at neighboring terrace levels interfere destructively. Hence intensity variations during the deposition process will mainly be due to a change in the relative size of the ''visible'' fractions of adjacent terrace levels. This information can be used to draw conclusions about growth modes.[18] On the other hand, if there is constructive interference (*in-phase* scattering), the dominant effect for intensity variation is *diffuse scattering* from surface defects like adatoms, vacancies, or step edges,[18,19] whose concentration change can be estimated by such an experiment.

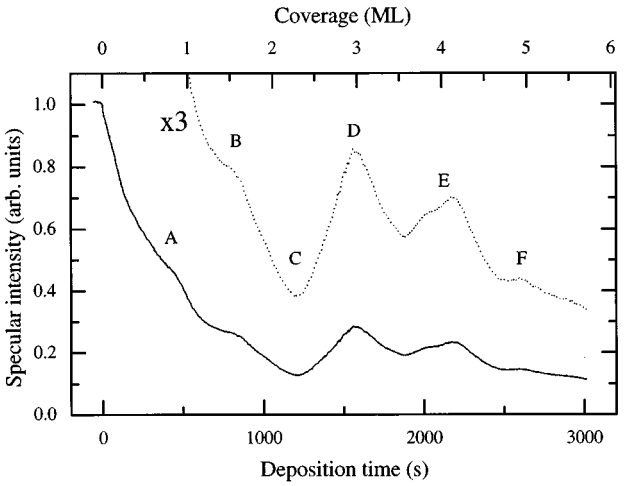

FIG. 2. Specular helium intensity as a function of Co coverage. The dotted curve is threefold enlarged. $R = 0.137$ ML/min, $\chi = 86.84°$, $E_i = 28.5$ meV, and $T = 300$ K.

For specular scattering, the phase difference

$$\varphi = 2k_i h \cos\vartheta_i \tag{1}$$

between two beams can be calculated from the wavenumber $k_i = 2\pi/\lambda = \sqrt{2mE_i}/\hbar$ of an incoming helium atom of energy E_i and mass $m \simeq 4u$, the step height h and the angle ϑ_i between the surface normal and the incoming beam. For $\varphi = 2\pi n$, integer n leads to in-phase scattering, half-integer n to antiphase scattering. Since we are dealing with heteroepitaxy, the choice for h is not evident: at the very beginning intrinsic substrate steps are present, whereas during deposition changes in step height are to be expected, and relaxation effects can cause substantial deviations of the measured step heights from those calculated using the bulk lattice constants.

Nevertheless, for the deposition curve of Fig. 2, we chose the antiphase condition for $h = 2.05$ Å, being the distance between two [0001] lattice planes in the hcp bulk Co at room temperature. This was achieved by adjusting the total scattering angle $\chi = 2\vartheta_i$ to 86.84°, such that, according to Eq. (1), $\varphi = 7\pi$ for $E_i = 28.5$ meV. The consequences of this choice for measurement analysis will be discussed below.

Figure 2 can now be interpreted as follows. At the beginning of the deposition we observe a steep decrease in the specular helium intensity which is due to the formation of small Co islands on the Au(111) surface. Depending on the actual interference condition, this can be due to destructive interference and/or to diffuse scattering at adatoms or step edges. With increasing deposition the absolute slope of the specular intensity decreases and two ''shoulders'' A and B appear which will be discussed below. They are followed by three damped oscillations D, E, and F. The distances DE and EF are equal and about one third of the distance of maximum D from the beginning of the deposition. Having chosen the antiphase condition to correspond to a single Co step, this suggests a periodical change in the ratio of the visible fractions of neighboring terrace levels, indicating layer-by-layer growth from the third to fifth layers. However, the intensities of the oscillation maxima lie far below the initial intensity ($I_0 = 1$) which would be expected to be recovered for *ideal* two-dimensional growth in a homoepitaxial system. Since we are dealing with heteroepitaxy, recovering the initial intensity is not expected because of the different helium reflectivity of the two materials. Furthermore, in view of the strong damping of the higher oscillations, we may infer that the growth is not ideally two dimensional, and that nucleation already takes place in the next layer before completion of the former one. Above 5 ML, no further oscillations are visible, so we conclude that the growth of thicker Co films is three dimensional. This interpretation of the deposition curve raises the question about the growth mechanism of the first three layers.

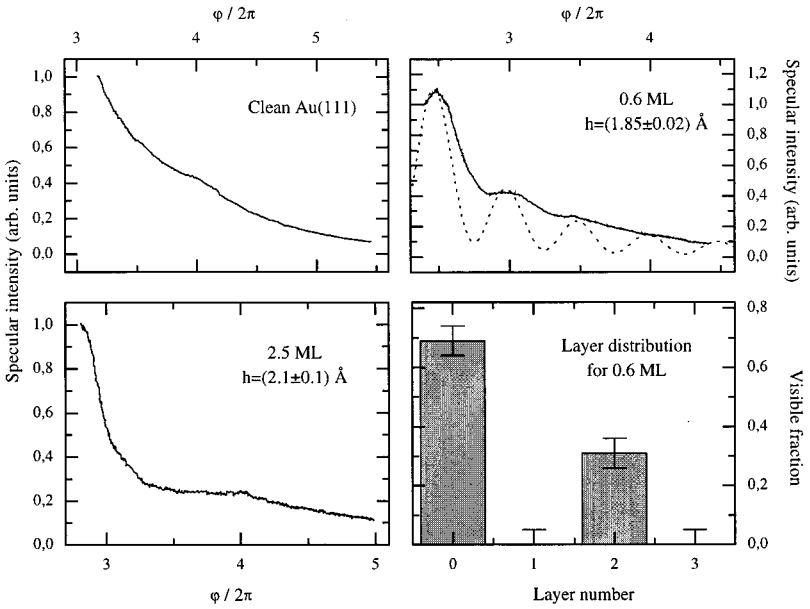

FIG. 3. Determination of layer distribution and step height by helium interference curves for various Co coverages. $E_i = 20 \ldots 70$ meV, $\chi = 90°$, and $T = 300$ K. (a) Clean Au(111), $h = 2.36$ Å. (b) $\Theta = 0.6$ ML, $h = (1.85 \pm 0.02)$ Å. (c) $\Theta = 2.5$ ML, $h = (2.1 \pm 0.1)$ Å. (d) Best-fit layer distribution extracted from (b) yielding the dotted curve in (b) as described in the text.

B. Step height of the Co islands

The layer distribution and the step height of the Co islands at different coverages can be examined by so-called *interference curves*. In this experiment, the specular helium intensity is detected as a function of the phase difference φ [Eq. (1)] by varying the helium wave number k_i through the variation of the helium nozzle temperature. Alternatively, φ could be varied by changing the total scattering angle $\chi = 2\vartheta_i$ while keeping k_i fixed—an experiment which is often referred to as *rocking curve*. Considering Eq. (1), it is evident that both experiments lead to a periodic change from in-phase (intensity maxima) to antiphase condition (intensity minima). These intensity oscillations may be superposed by a continuous attenuation of the specular intensity with increasing $k_{i\perp} = k_i \cos\vartheta_i$ due to the *Debye-Waller effect*.[20]

Figures 3(a)–3(c) show helium interference curves for several Co coverages on the Au(111) surface. The x axis has been rescaled from E_i to φ by Eq. (1) using the best-fit step height h. Figure 3(a), taken from the clean Au(111) surface ($h = 2.36$ Å), exhibits only one weak oscillation indicating that the average terrace width is rather large compared to the transfer width[21] of the apparatus (≈ 300 Å). Upon Co deposition, several oscillations become apparent [Fig. 3(b)]: at a coverage of 0.6 ML three equidistant maxima are visible. A simple model assuming the coherent overlap of plane waves emerging from different terrace levels can be used to calculate the intensities,[22]

$$\frac{I}{I_0}(k_i) = e^{-\alpha k_i^2} \left| \sum_{j=0}^{\infty} a_j e^{-ij\varphi(k_i)} \right|^2 . \qquad (2)$$

Herein, I_0 is the intensity that would be measured for a flat (unstepped) surface, $\varphi(k_i)$ is the phase shift [see Eq. (1)], and a_j the visible fraction of terrace level j. The exponential prefactor accounts for the intensity attenuation due to the Debye-Waller effect. The dotted curve in Fig. 3(b) has been calculated using Eq. (2), and rescaled to φ as abscisse. The corresponding best-fit layer distribution is displayed in Fig. 3(d).

The step height deduced from the position of the intensity maxima in Fig. 3(b) using Eq. (2) is $h = (3.70 \pm 0.03)$ Å . This value is much too large for a monatomic step, which is expected to lie somewhere between $h = 2.05$ Å for Co(0001) and $h = 2.36$ Å for Au(111), but somewhat smaller than for a double step (4.10 Å for double Co and 4.41 Å for a Co-Au step). Nevertheless, we may conclude that Co double-layer islands are formed. The remaining deviation can be attributed to surface relaxation effects, e.g., at the Au-Co and Co-Co interfaces. These are to be expected rather than a surprise, because of the double-layer growth in this coverage regime. In addition, helium scattering does not measure the true ''geometric'' step height but the difference between classical ''turning points'' of helium atoms above the surface, so the different interaction potential between helium atoms and gold or cobalt layers, respectively, could also be responsible for the observed lower value. Another possible contribution may be due to the *Smoluchovski effect*: if the average terrace width is very small, the corrugation function probed by the helium atoms is effectively smoothed, such that the step height measured by TEAS is smaller than the true geometric step height as measured, for instance, by low energy electron diffraction with spot profile analysis (SPALEED).[23] In STM experiments under similar experimental conditions, a value $h = 4.10$ Å close to the double Co(0001) bulk step height[11] was observed.

The best-fit layer distribution displayed in Fig. 3(d) shows almost perfect double-layer islands, although slight nucleation on the islands cannot be completely excluded [error bars in Fig. 3(d)]. The shape of the interference curve in Fig. 3(b) does not considerably change up to about 2.5 ML [Fig. 3(c)]. Here, the best-fit step height is (2.1 ± 0.1) Å, which is in good agreement with the expected geometric height of a monatomic Co(0001) step (2.05 Å). The quality of this measurement, however, is too poor to allow a detailed analysis of the layer distribution. Above 2.5 ML, no further change in step height could be observed. This is consistent with a quasi-2D growth of monatomic layers as deduced from deposition curves (Fig. 2) for this coverage regime in Sec. III A.

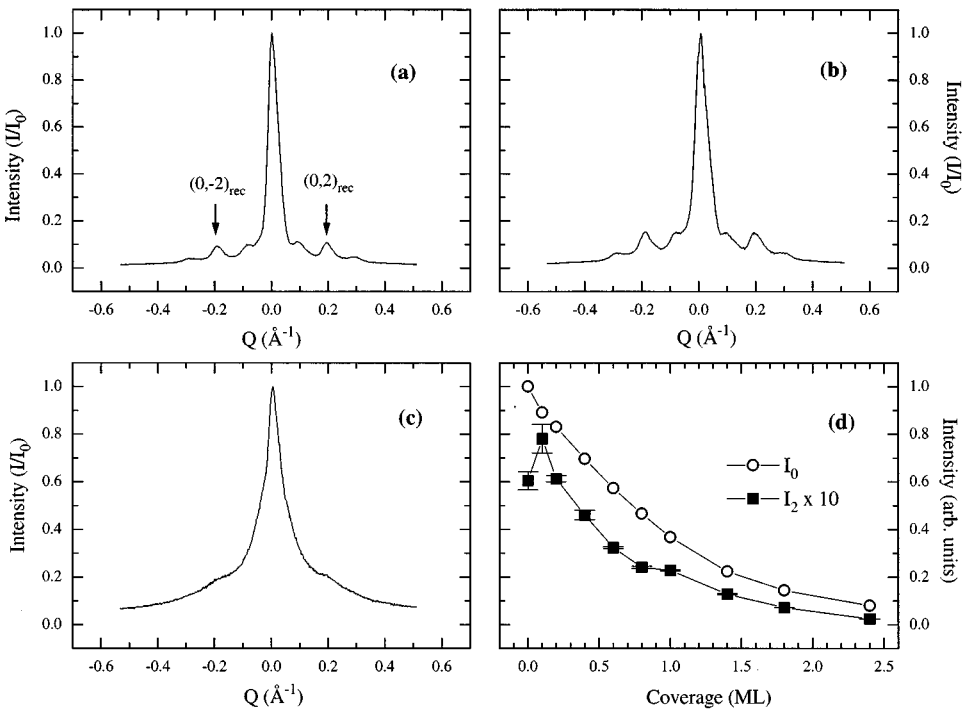

FIG. 4. Helium diffraction profiles at various Co coverages. $E_i = 25.0$ meV, $\chi = 87.88°$, [110] direction. (a) Clean Au(111). (b) $\Theta = 0.1$ ML. (c) $\Theta = 2.4$ ML. (d) Intensity of selected diffraction peaks as a function of Co coverage (see text). The Lorentzian-shaped background has been subtracted.

At this point, it should be mentioned that Speckmann, Oepen, and Ibach found evidence of gold-''capped'' Co structures using AES upon annealing about 2–3-ML Co/Au(111) deposited at 300–600 K, and cooling back to room temperature.[12] At room temperature, the surface free energies are such that in thermodynamic equilibrium one would expect that Au completely wets the Co nanostructures.[24] From our experiments conducted at room temperature, there is no direct evidence of such Au capping. In fact, the Au-Co-Au step ($h = 4.41$ Å) should be even higher than the Co double-layer step ($h = 4.10$ Å). On the other hand, we have seen that surface relaxation and other effects indeed may be quite important, so this scenario cannot be completely ruled out. Also, there could be a partial exchange between Co and Au leading to a surface confined mixture. Further experiments are currently underway to clarify this question on the surface composition.

C. Preferential nucleation at the reconstruction elbows

To investigate the island distribution in the initial stage of Co epitaxy, helium diffraction profiles along the [110] direction for various Co coverages on the Au(111) surface were recorded [Figs. 4(a)–4(c)]. They were obtained by varying the angle of incidence ϑ_i while keeping χ fixed; the intensity is then plotted as a function of the wave-vector transfer parallel to the surface, which is related to the angles ϑ_i and ϑ_f through

$$Q = k_i(\sin\vartheta_i - \sin\vartheta_f), \tag{3}$$

with $\vartheta_f = \chi - \vartheta_i$. Profile (a) recorded from the clean Au(111) surface exhibits several diffraction peaks in the vicinity of the specular beam that are due to the Au(111) reconstruction described above: the distance of these peaks in reciprocal space corresponds to $L_D \simeq 63$ Å in real space (Fig. 1).

Surprisingly, upon Co deposition the diffraction intensities of the superstructure peaks are just enhanced [Fig. 4(b)]. We conclude that the corrugation amplitude of the reconstruction is increased by the deposition, i.e., Co atoms must have nucleated at particular sites of the reconstruction pattern, thereby replicating the original superstructure periodicity. Indeed, STM studies have shown that Co preferentially nucleates at the ''elbows'' of the Au(111) reconstruction. This can be rationalized in view of the large lattice misfit of about -14% between Co(0001) and Au(111) (bulk values). Since the lattice of the ideal Au(111) surface is substantially distorted in the vicinity of the reconstruction elbows, these sites could be energetically favored for nucleation of adsorbates exhibiting a large lattice misfit. A similar behavior has been observed for nickel[13] and iron[14] on Au(111). In contrast to these systems, the nucleation of adsorbates with small lattice misfit with respect to the Au(111) substrate such as gold itself,[13] silver,[25] or aluminum[26] was not found to preferentially occur at the reconstruction elbows.

For a more detailed analysis the Lorentzian-shaped diffuse background has to be subtracted from the diffraction profiles. Figure 4(d) shows the resulting specular intensity I_0 and the average intensity I_2 of the two second-order reconstruction peaks in [110] direction [$Q = \pm 0.19$ Å^{-1}; see Fig. 4(a)] as a function of Co coverage. The error bars represent the difference in peak height of the $(0,2)_{\text{rec}}$ and the $(0,2)_{\text{rec}}$ beam. It is clearly visible that after an initial rise further Co deposition leads to a continuous attenuation of I_2, which means that the influence of the reconstruction network on the surface morphology becomes less pronounced. However, at a coverage of 2.4 ML [Fig. 4(c)], the reconstruction peaks are still discernible: the reconstruction of the substrate influences the surface morphology even at these higher Co coverages. It should be noted that both position and half-width of the reconstruction peaks remain constant as long as they are detectable.

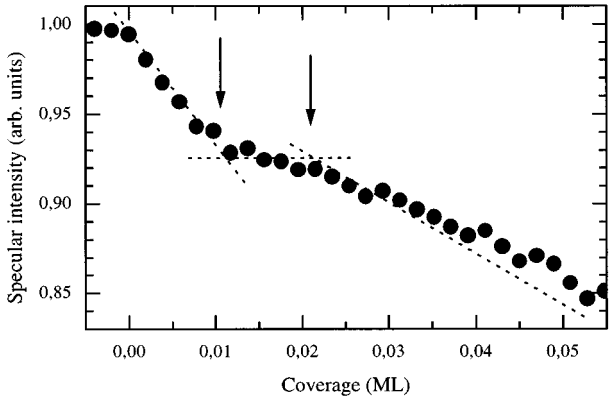

FIG. 5. Specular helium intensity as a function of Co coverage. $E_i = 26.9$ meV, $\chi = 90°$, $T = 300$ K, and $R = 0.078$ ML/min.

If we take a closer look at the very beginning of a Co deposition curve (Fig. 5), we can obtain further insight into the nucleation process at the reconstruction elbows. When opening the shutter the specular intensity initially drops very rapidly due to scattering at small Co clusters. For helium atoms, these clusters act like stains on a perfect mirror, which means that helium atoms that impinge on such a small cluster are scattered diffusely, and do not contribute to the specular intensity. From the slope of the curve at the beginning of the deposition we can calculate the effective cross section Σ for diffuse scattering per atom in the cluster,[27]

$$\Sigma = -\frac{1}{n_s I_0}\left.\frac{dI}{d\Theta}\right|_{\Theta=0}, \tag{4}$$

where $n_s = 0.139$ Å^{-2} denotes the atom density of the Au(111) surface, and I_0 the specular intensity of the clean surface. The observed value is $\Sigma \approx 90$ Å^2, which is roughly one order of magnitude larger than the geometric size of the atom in a 2D solid Co cluster. This appears to be a general feature of point defects like adatoms or vacancies on metal surfaces.[18] However, one has to be very careful when evaluating Eq. (4), because we are not dealing with *homogeneous* nucleation on a *flat* surface. Equation (4) under these conditions gives the effective cross section for one atom in the *stable nucleus*,[28] a quantity that is not defined for *heterogeneous* nucleation because the density of the nuclei is predefined by the density of the preferred nucleation sites, i.e., the reconstruction elbows. Since we do not know how many atoms are necessary to form a stable cluster at an elbow site, we do not know the exact cluster size to which the observed value of Σ refers to. Furthermore, the extrapolation of $dI/d\Theta$ to $\Theta = 0$ can only be done reasonably down to $\Theta \approx 0.002$ ML, where on average 3–4 Co atoms should have already reached an elbow (assuming that all deposited Co atoms have migrated to an elbow). Since Σ is of the same order of magnitude as for single adatoms on unreconstructed (111) surfaces,[18,29] we can conclude that the deformation of the helium-surface interaction potential by Co nucleation at the elbows is even larger than, e.g., for Pt/Pt(111).

At a coverage of about 1% of a monolayer, the deposition curve exhibits a kink, and during the following 1% of a monolayer the specular intensity hardly decreases. Then, another kink is observed at 0.02 ML and the intensity drops again, but with a slope only half the initial one. This can be interpreted as follows.

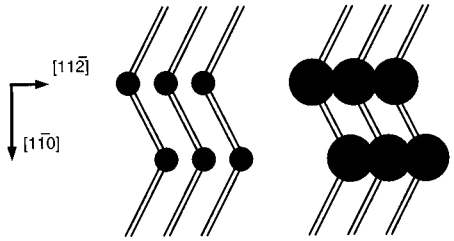

FIG. 6. Model of the nucleation and growth of submonolayer amounts of Co.

The first deposited Co atoms nucleate at the elbows of the Au(111) reconstruction forming small clusters with monatomic step height. Assuming that all atoms can diffuse to the elbows an average size of 15–20 atoms per elbow can be estimated for the ''kink'' coverage of 0.01 ML. At this point the specular intensity decay is strongly reduced, i.e., the following Co atoms hardly increase the diffusely scattering area. This can be explained by the formation of a second layer on top of the clusters. Above 0.02 ML, the Co islands grow laterally with double Co step height. Since now the double amount of Co is necessary to create the same diffusely scattering area such as that just below 0.01 ML, it is clear that the slope of the deposition curve just above 0.02 ML is only half the initial one.

With the above results we can also explain the occurrence of the ''shoulders'' *A* and *B* of the deposition curve in Fig. 2. As we have stated above, Co atoms nucleate preferentially at the elbows of the Au(111) reconstruction as shown schematically in Fig. 6. Assuming that these islands are of compact shape (as shown by STM in 11), e.g., disk shaped, we can easily calculate that, for isotropic growth double-height islands should coalesce at a coverage of 0.72 ML forming ''chains'' along the [112] direction (Fig. 6). This corresponds to the coverage at which shoulder *A* is observed in Fig. 2, leading to the conclusion that the coalescence of the islands diminishes the step length per unit area resulting in a reduced diffusely scattering area. Since in this coverage regime double-layer Co islands are present on the surface, the actual interference condition is close to in-phase scattering [recall that we chose antiphase for the nominal Co single step height, and thus automatically in-phase for the nominal Co double step height; see Eq. (1)]. Hence the dominant effect for intensity variation is diffuse scattering.

The interpretation of shoulder *B* ($\Theta = 1.5$ ML) is then straightforward: the Co chains grow perpendicularly to their axis, and coalesce again. Since nucleation on the chains cannot be neglected, a more detailed analysis of the surface morphology at the coverage in *B* is quite difficult. It is worth mentioning that the antiphase condition for Co single steps realized in Fig. 2 is perfectly suited for growth analysis of this system: below about 2.5 ML, Co double layers lead to *in-phase* condition resulting in high sensitivity for diffuse scattering which enables the observation of the kinks *A* and *B* (see Sec. III B). Above 2.5 ML, the antiphase condition for Co single steps is the best choice for detection of the growth mode (i.e., the quasi-2D growth of layers 3–5). Indeed,

deposition curves recorded at different scattering conditions did not reveal any additional information on this system throughout the measured coverage range.

IV. CONCLUSION

Cobalt deposition on the reconstructed Au(111) surface at room temperature leads to the formation of small Co clusters at the ''elbows'' of the reconstruction. Growing initially with monatomic step height, these islands cease to expand laterally at an average cluster size of about 15–20 atoms. After the second layer is formed on the islands they grow laterally with double Co(0001) step height. At about 0.7 ML the islands coalesce along the [112] direction, forming chains which finally coalesce along the [110] direction perpendicularly to their axis at about 1.5 ML. At 2.5 ML, we observed monatomic Co step heights, and the third to fifth layers grow in quasi-two-dimensional fashion.

[1] Science **254**, 1300 (1991).
[2] C. F. Quate, in *Highlights in Condensed Matter Physics and Future Prospects*, edited by L. Esaki (Plenum, New York, 1991).
[3] L.-W. Lyo and P. Avouris, Science **253**, 173 (1991).
[4] D. M. Eigler, C. P. Lutz, and W. E. Rudge, Nature **352**, 600 (1991).
[5] P. Zeppenfeld, C. P. Lutz, and D. M. Eigler, Ultramicroscopy **42/44**, 128 (1992).
[6] M. Sundaram, S. A. Chalmers, P. F. Hopkins, and A. C. Gossard, Science **254**, 1326 (1991).
[7] D. D. Chambliss, R. J. Wilson, and S. Chiang, Phys. Rev. Lett. **66**, 1721 (1991).
[8] D. Renard and G. Nihoul, Philos. Mag. B **55**, 75 (1987).
[9] C. Chappert *et al.*, J. Magn. Magn. Mater. **54-57**, 2 (1986).
[10] T. Kingetsu and K. Sakai, J. Appl. Phys. **74**, 6308 (1993).
[11] B. Voigtländer, G. Meyer, and N. M. Amer, Phys. Rev. B **44**, 10 354 (1991).
[12] M. Speckmann, H. P. Oepen, and H. Ibach, Phys. Rev. Lett. **75**, 2035 (1995).
[13] D. D. Chambliss, R. J. Wilson, and S. Chiang, J. Vac. Sci. Technol. B **9**, 933 (1991).
[14] B. Voigtländer, G. Meyer, and N. M. Amer, Surf. Sci. **255**, L529 (1991).
[15] K. E. Kuhnke, Ph.D. thesis, Universität Bonn, 1991.
[16] A. R. Sandy *et al.*, Phys. Rev. B **43**, 4667 (1991).
[17] J. V. Barth, H. Brune, G. Ertl, and R. J. Behm, Phys. Rev. B **42**, 9307 (1990).
[18] B. Poelsema and G. Comsa, *Scattering of Thermal Energy Atoms*, Springer Tracts in Modern Physics Vol. 115 (Springer, Berlin, 1989).
[19] B. Poelsema *et al.*, Surf. Sci. **272**, 269 (1992).
[20] V. Bortolani *et al.*, Surf. Sci. **208**, 1 (1989).
[21] G. Comsa, Surf. Sci. **81**, 57 (1979).
[22] M. A. Krzyzowski, C. Romainczyk, P. Zeppenfeld, and G. Comsa (unpublished).
[23] P. Bedrossian *et al.*, Surf. Sci. **334**, 1 (1995).
[24] S. Blügel (private communication).
[25] M. M. Dovek, C. A. Lang, J. Nogami, and C. F. Quate, Phys. Rev. B **40**, 11 973 (1989).
[26] H. Hannemann *et al.* (unpublished).
[27] G. Comsa and B. Poelsema, Appl. Phys. A **38**, 153 (1985).
[28] J. A. Venables, J. D. T. Spiller, and M. Hanbücken, Rep. Prog. Phys. **47**, 399 (1984).
[29] M. A. Krzyzowski, Ph.D. thesis, Universität Bonn, 1995.
[30] L. Huang (private communication).